Theoretical Performance of Rocket and Turbojet Engines Operating in the Continuous Detonation Mode

Dmitry DAVIDENKO, Yohann EUDE,* Iskender GÖKALP,* and François FALEMPIN***
**ICARE – CNRS*
1C Avenue de la Recherche Scientifique, 45071 Orléans, France
***MBDA France*
1 Avenue Réaumur, 92358 Le Plessis Robinson, France

Abstract
Performance of a hydrogen-oxygen rocket engine and a kerosene-fuelled turbojet is analyzed for the conventional constant-pressure combustion mode and the continuous detonation wave mode. Flow parameters in main cross sections and engine performance are evaluated using global 0D engine models with detailed thermochemical description of equilibrium combustion products. Performance results are obtained in wide ranges of engine operation parameters. It is shown that the continuous detonation mode has an important advantage over the constant-pressure mode for both engines.

1. Introduction

Superiority of the detonation-based thermodynamic cycle was theoretically proven by Zeldovich for the first time [1]. The analysis of engine cycles, proposed by Wintenberger and Shepherd [2], demonstrates that the detonation (Fickett-Jacobs) cycle provides the highest efficiency with respect to the constant-pressure (Brayton) and constant-volume (Humphrey) cycles.
Among known concepts, the concept of Continuous Detonation Wave Engine (CDWE) is chosen to analyze its applications as a rocket (CDWRE) or a turbojet (CDWTJ). The Fickett-Jacobs cycle can be considered as a limiting case of the CDWE cycle assuming that the detonation propagates under the total conditions just after the compression stage. A more realistic approach consists in assuming some expansion during the mixture admission into the chamber.
Since the pioneering works of Voitsekhovsky [3, 4] in Russia as well as Nicholls and Cullen [5] in the USA in 1950-60-s, which proved the feasibility of continuous detonation wave mode, interest in practical applications of CDWE has been rather limited during several decades. Today, with the rise of concern in more efficient principles of energy conversion, CDWE becomes attractive.
For practical application, the superiority of a CDWE over a conventional engine must be finally demonstrated with an engine prototype. However a first important step consists in comparing the theoretical potential of both engines.
First theoretical estimations of CDWRE performance are known from the report by Nicholls and Cullen [5] and the paper by Adamson and Olsson [6]. The calorically perfect gas approach was used assuming constant but different properties for the fresh mixture and combustion products. The combustion chamber was considered together with a convergent-divergent nozzle providing a sonic throat. These estimations resulted in the following conclusion [6]: "the ideal performance of an RDWE[1] is essentially the same as that of a conventional rocket engine, as long as the average chamber conditions are the same, for the same propellant mixture." It should be noted that the pressure at the nozzle exit and the nozzle area ratio were supposed the same for both engines. Hence the advantage of CDWRE could be realized only though the difference of the sound speeds in combustion products, which was found practically negligible. A different basis for the performance comparison should be chosen to avoid this misleading conclusion.
Later estimations of the performance of a CDWRE chamber are known from the papers of Bykovskii and Mitrofanov [7] and Bykovskii et al. [8]. In these estimations, the same constant thermodynamic properties were assumed for the fresh mixture and the combustion products. The combustion chamber was considered without cross section restriction allowing for supersonic flow at its exit. According to [8], a constant-area combustor operating in CDWRE mode provides a 7-18 % higher specific impulse at its exit than the same combustor operating in deflagrative

[1]Means CDWRE in the present paper.

combustion mode. This performance comparison demonstrates superiority of a CDWRE over a conventional rocket engine (CRE) but it is not sufficient if applied to a propulsion system because it does not take into account the flow expansion in the nozzle.
The present work is aimed at evaluation of the theoretical potential of CDWRE and CDWTJ with respect to the conventional engines. Global performance models of both engines are developed in the frame of this study. A detailed comparative study on rocket engine performance for the constant-pressure and continuous detonation modes has been already published in [9]. The present paper provides main results related to the rocket engine and a similar analysis for the turbojet.

2. Engine models

Physicochemical processes in an engine are quite complex and detailed simulation of a complete flowfield is too costly. In this work, engine performance is estimated using a global 0D approach, which is based on the following simplifying assumptions:
– chemically frozen composition for the propellants and chemical equilibrium for the combustion products;
– complete mixing and combustion of the propellants;
– uniform flow in the cross sections where the flow state is determined;
– absence of losses excepting some specific elements mentioned below;
– steady-state engine operation.
In the present work, the thermochemical model is limited to the gas-phase with either frozen or chemically equilibrium composition. Individual chemical species are considered as thermally perfect ideal gases with temperature-dependent thermodynamic properties. Any thermodynamic property of the gas mixture can be determined from the species properties for given pressure, P, temperature, T, and species mass fractions, $\mathbf{Y} = \{Y_s, s \in [1, N_s]\}$, using classical mixing laws [10]. The ideal gas law is used as the equation of state for the gas mixture. Among available chemical equilibrium solvers, the STANJAN code [11] is chosen to compute the chemical composition and mixture properties.
In any cross section, gas flow properties can be evaluated from the known state at the previous section using a set of equations that express basic relations for the mass flow rate, flow momentum, and flow enthalpy. Specific terms can be introduced in these equations to represent mass, momentum and energy exchange due to the fuel addition, cross section change, and mechanical work. In some cases, it is more convenient to use isentropic relations instead of the momentum equation. In particular, the following relations link static and total conditions of a gas flow:

$$s(P, T, \mathbf{Y}) = s(P_\mathrm{t}, T_\mathrm{t}, \mathbf{Y}_\mathrm{t}) \tag{1}$$

$$h(P, T, \mathbf{Y}) + \tfrac{1}{2}u^2 = h(P_\mathrm{t}, T_\mathrm{t}, \mathbf{Y}_\mathrm{t}) \tag{2}$$

where s is the entropy; h is the enthalpy; u is the flow speed; subscript "t" denotes the total or stagnation conditions. In the case of frozen composition, $\mathbf{Y} = \mathbf{Y}_\mathrm{t}$ whereas, for the equilibrium composition, $\mathbf{Y} = \mathbf{Y}(P, T)$ and $\mathbf{Y}_\mathrm{t} = \mathbf{Y}_\mathrm{t}(P_\mathrm{t}, T_\mathrm{t})$. From (1) and (2), it can be stated that the total parameters of an isentropic adiabatic flow remain constant.
Given that the temperature-dependent species properties are specified by nonlinear functions and the equilibrium state is determined by a numerical procedure, it is not possible to obtain explicit analytical relations between the flow states. Instead numerical methods must be used to determine the flow state at each section.

2.1 Conventional rocket engine model

The following parameters are prescribed for the CRE model: chemical composition for oxidizer and fuel; mixture ratio or oxidizer-to-fuel mass ratio, f; total injection parameters, P_tj and T_tj; injected mass flow rate, G_j; chamber cross-section area, A_c, which is assumed infinitely large; and nozzle exit pressure, P_e. Flow conditions in the main cross sections are determined as follows:
1) Fresh mixture ("m"): Assuming no hydrodynamic losses and a non-reacting propellant mixture in this section, it is possible to write $P_\mathrm{tm} = P_\mathrm{tj}$ and $T_\mathrm{tm} = T_\mathrm{tj}$. For an infinitely large cross section, the mixture velocity is 0 and the mixture static parameters are equal to the total ones.
2) Combustion products ("c"): From this section, the gas is represented by equilibrium combustion products. As in the previous section, the flow speed is 0, and one can find from the momentum equation $P_\mathrm{tc} = P_\mathrm{tm}$. In the present model, the heat of formation is included in the enthalpy of chemical species, hence the total enthalpy is preserved, and the total temperature can be found from the equality $h(P_\mathrm{tm}, T_\mathrm{tm}, \mathbf{Y}_\mathrm{tm}) = h(P_\mathrm{tc}, T_\mathrm{tc}, \mathbf{Y}_\mathrm{tc})$.

3) Sonic throat ("th"): From the "c" section, the flow is assumed isentropic hence the total conditions, determined in the previous cross section, are preserved. Equations (1) and (2) and the sonic flow condition are used to calculate the static parameters of the flow. The cross-sectional area is determined as $A_{th} = G_j/(\rho_{th}\, u_{th})$, ρ_{th} being the density.
4) Nozzle exit ("e"): The solution procedure is analogous to the "th" section but, instead of sonic flow condition, the prescribed pressure, P_e, is used to determine the static parameters and the flow speed.

2.2 Conventional turbojet model

The following parameters are prescribed for the CTJ model: chemical composition for fuel; fuel equivalence ratio, ϕ; flight speed, u_a; total parameters at the inlet, $P_{t\,in}$ and $T_{t\,in}$; compressor pressure ratio, π_{co}, and compressor efficiency, η_{co}; total pressure recovery, σ_c, in the combustion chamber; turbine efficiency, η_{tu}; mechanical efficiency of the compressor-turbine transmission, η_{tr}; air mass flow rate, G_a; cross-section areas, A_{in}, A_{co}, A_c, A_{tu}; and nozzle exit pressure, P_e. Flow conditions in the main cross sections are determined as follows:

1) Compressor exit ("co"): The total pressure is determined as $P_{t\,co} = P_{t\,in}\,\pi_{co}$. The compressor work results in increase of the air total enthalpy according to the formula $h_{t\,co} = h_{t\,in} + (h^s_{t\,co} - h_{t\,in})/\eta_{co}$, where $h^s_{t\,co}$ is the enthalpy of isentropically compressed air from the "in" state to a state defined by $P_{t\,co}$. The total temperature is defined by the relation $h_{t\,co} = h(T_{t\,co}, \mathbf{Y}_a)$, where $\mathbf{Y}_a$ represents the chemical composition of air.
2) Combustion products ("c"): From this section, the gas is represented by equilibrium combustion products. The total pressure is determined as $P_{t\,c} = P_{t\,co}\,\sigma_c$. The total enthalpy of combustion products is given by the relation $h_f\, G_f + h_{t\,co}\, G_a = h_{t\,c}\, G_g$, where h_f and G_f are respectively the enthalpy and mass flow rate of fuel, and $G_g = G_a + G_f$ is the mass flow rate of gases. The corresponding total temperature must satisfy the equality $h_{t\,c} = h(P_{t\,c}, T_{t\,c}, \mathbf{Y}_{t\,c})$.
3) Turbine exit ("tu"): In the turbine, the gas total enthalpy decreases, and the resulting work is transmitted to the compressor providing the following relation $h_{t\,tu} = h_{t\,c} - (h_{t\,co} - h_{t\,in})\, G_a/(G_g\, \eta_{tr})$. The total pressure, $P_{t\,tu}$, is found from an isentropic expansion from the "c" state to a state defined by the enthalpy $h^s_{t\,tu} = h_{t\,c} - (h_{t\,c} - h_{t\,tu})/\eta_{tu}$. The total temperature must satisfy the condition $h_{t\,tu} = h(P_{t\,tu}, T_{t\,tu}, \mathbf{Y}_{t\,tu})$.
4) Sonic throat ("th") and nozzle exit ("e"): The computational procedure is analogous to that described for the rocket engine model.

In any cross section, speed and static parameters of the flow are obtained from known total parameters, mass flow rate, and cross-section area.

2.3 Engine models for the continuous detonation mode

The operation principle of a CDWE chamber is described and illustrated in [12, 13]. The reader can find numerical results from 3D simulations in these papers as well as 2D computational results in [14, 15] looking for information on the flow structure and some integral characteristics of the flowfield. Briefly, CDWE chamber operation can be described as follows. A mixture of fuel and oxidizer is injected at one end of an annular cylindrical chamber thus creating a layer of combustible mixture near the injection head. After detonation initiation, one or more detonation fronts, normal to the injection surface, will propagate in the azimuthal direction consuming the continuously growing layer of fresh mixture. Combustion products, generated by detonation waves, expand and are exhausted through the other end of the chamber.

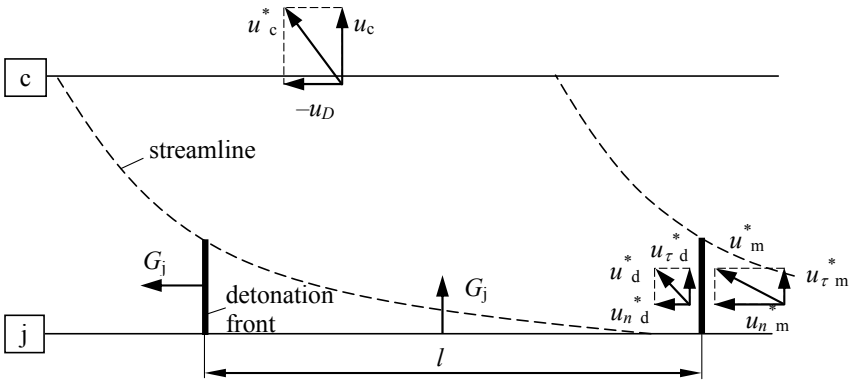

Figure 1: Schematic of the periodic flow structure in a CDWE combustion chamber

Particularities of the continuous detonation mode are related to the combustion chamber description. Schematic representation of the flow structure in a CDWE chamber is shown in Fig. 1. Fresh mixture of fuel and oxidizer is injected normal to the "j" plane. The streamline contours delimit flow tubes passing through individual detonation fronts. It is assumed that the detonation waves propagate along the injection plane at a constant velocity, u_D, and with a constant spatial period, l, providing that the flowfield in the chamber is periodic. Sections "j" and "c" delimit the zone, in which the flow is considered in two reference frames: the fixed frame (FF) and the moving frame (MF) attached to a detonation. The flow velocity in MF is marked with asterisk. In MF the flowfield is considered steady state. Due to multidimensional flow structure, the gas state is nonuniform between two successive detonations. The "m" section represents the fresh mixture state just in front of the detonation. The "d" section is introduced for the flow state in the Champan-Jouguet (CJ) plane.

Flow conditions in the "m" section are determined from prescribed total injection conditions and Mach number, M_m, in FF. The latter is used as a model parameter. Assuming no losses at mixture injection, the total state in FF is defined as $P_{t\,m} = P_{t\,j}$ and $T_{t\,m} = T_{t\,j}$. For simplicity it is assumed that $u_{n\,m} = 0$ and $u_{\tau\,m} = u_m$. Indeed the results of 2D simulations [14, 15] show that the mean value of $u_{n\,m}$ is relatively small and can be neglected in comparison with the detonation velocity.

To determine the flow state in the "d" section, the following hypotheses are accepted:

– the detonation front is flat and normal to the injection plane;
– the detonation propagates in the CJ regime in the fresh mixture;
– the injected mixture does not mix with the combustion products prior the detonation;
– all the injected mixture is burnt in detonation waves.

The second assumption allows writing the following relations for the normal velocity components:

$$u^*_{n\,m} = D_{CJ} \quad \text{and} \quad u^*_{n\,d} = c_d \tag{3}$$

where D_{CJ} is the CJ detonation velocity; c_d is the sound speed in section "d". Assuming that the reaction zone length in the detonation is negligible, it is possible to equate the tangential velocity components as $u^*_{\tau\,m} = u^*_{\tau\,d}$.

The CJ conditions (section "d") in MF are determined using conditions (3) and the equations of mass, momentum and total enthalpy written for the normal velocities $u^*_{n\,m}$ and $u^*_{n\,d}$.

One must take additional assumptions to determine the flow state at the chamber exit (section "c"). By assuming that the shocks induced by detonations and the viscous losses due to flow shear are weak, the expansion process between sections "d" and "c" is considered isentropic thus allowing to set $P^*_{t\,c} = P^*_{t\,d}$. and $T^*_{t\,c} = T^*_{t\,d}$. Neglecting the skin friction on the chamber walls, the flow velocity at the chamber exit can be supposed axial in FF. Static state parameters are determined from Eqs. (1) and (2) for known $P^*_{t\,c}$, $T^*_{t\,c}$, and $u^*_c = (u_c^2 + D_{CJ}^2)^{1/2}$. Finally the total state at the chamber exit in FF is determined from the static state and the flow velocity, u_c.

Multidimensional expansion process in a constant-area chamber results in a supersonic flow at the chamber exit. Thus the chamber can be followed by a diverging nozzle without geometrical throat. Nevertheless, a sonic throat section is introduced in the CDWE models for compatibility with the conventional engine models.

2.4 Engine performance definition

Internal thrust of a rocket engine (RE) or a turbojet (TJ) in atmosphere is defined as follows:

$$F^{RE} = G_j u_e + (P_e - P_a) A_e, \quad F^{TJ} = G_g u_e - G_a u_a + (P_e - P_a) A_e \tag{4}$$

where P_a is the atmospheric pressure.

The engine specific impulse is determined as:

$$I^{RE}_{sp} = F^{RE} / G_j, \quad I^{TJ}_{sp} = F^{TJ} / G_f \tag{5}$$

Turbojet performance is more often characterized by the thrust-specific fuel consumption, which can be expressed in kg/N-h according to the following definition:

$$C^{TJ}_F = 3600 / I^{TJ}_{sp} \tag{6}$$

3. Performance analysis

3.1 H_2-O_2 rocket engine

A H_2-O_2 rocket engine is considered in this study. The thermochemical model of reacting H_2-O_2 mixture includes 6 species (H_2, O_2, H, O, OH, and H_2O). Both propellants are assumed at the same injection temperature T_{tj} = 300 K. The injection pressure, P_{tj}, ranges from 1 to 10 MPa. The mixture ratio, f, is varied from 4 to 13 corresponding to the range of fuel equivalence ratio from 2 to 0.6. The stoichiometric mixture ratio is approximately 7.94. For the CDWRE model, the Mach number in fresh mixture, M_m, is taken equal to 0.5. Results of 2D simulations [14, 15] for uniformly distributed injection show that M_m increases across the fresh mixture layer being around 0.5 in the middle and about 1 near the edge. Two pressure levels at the nozzle exit are considered: 100 kPa for sea-level operation and 1 kPa for nearly-vacuum operation. Full flow expansion is assumed in the nozzle providing $P_e = P_a$.

Before considering results on the overall engine performance, it is instructive to compare the evolution of gas state in P-v and T-s coordinates representing CRE and CDWRE processes. Corresponding diagrams are shown in Fig. 2 for the following conditions: f = 6, P_{tj} = 5 MPa, P_e = 100 kPa. The points in the graphs mark gas states in the main cross sections with corresponding designations. Log scale is used in the P-v diagram because of large ranges of pressure and specific volume variation. Points "j" and "m" coincide for CRE as the fresh mixture is assumed at rest. For CDWRE, point "m" represents static conditions before detonation at M_m = 0.5. For CRE, combustion takes place at constant pressure (segment "m"-"c"). For CDWRE, the detonation process is represented by "m"-"d" and the following expansion by "d"-"c". Point "d" represents static conditions after detonation whereas "c" – total conditions at the chamber exit. In linear P-v coordinates, segment "m"-"d" is a straight line called Reyleigh line [16]. In detonation, the initial mixture compression, corresponding to the von Neumann spike, is stronger so the process goes beyond point "d" but during combustion the flow state returns to "d" following the same straight line without any contribution to the cycle work. Segments "m"-"c" and "m"-"d" in T-s coordinates are traced arbitrarily as straight lines. From "d" to "c" then to "th" and "e", the isentropic process follows a power law in P-v coordinates and a vertical straight line s = const in T-s coordinates. Points "th" and "e" represent static conditions in the sonic throat and at the nozzle exit. From the P-v diagram, one can see that the CDWRE cycle produces extra work due to the area delimited by lines "m"-"c" for CRE and "m"-"d"-"c"-"th"-"e" for CDWRE. Results in the T-s diagram correspond to the Zeldovich theory [1] that a detonation-based cycle generates less entropy as compared to any other cycle starting from the same initial conditions.

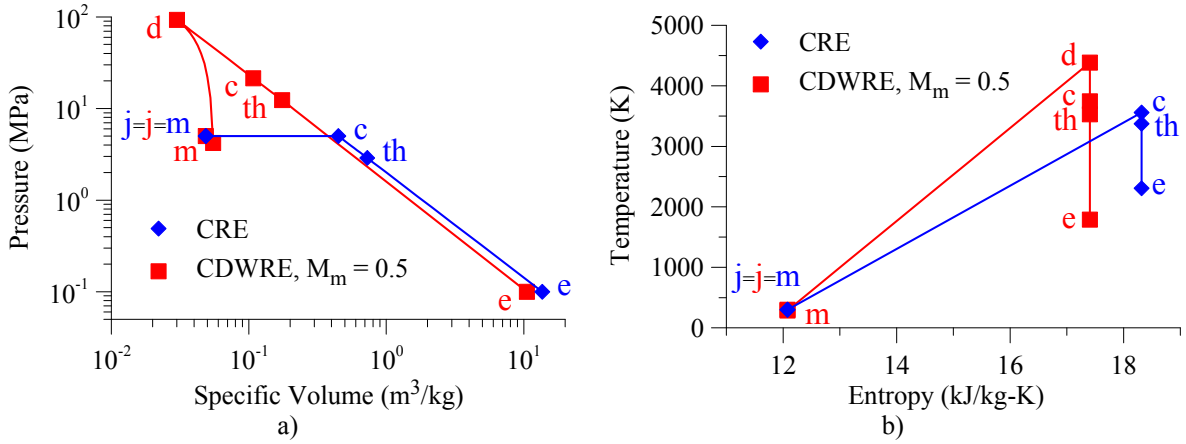

Figure 2: P-v (a) and T-s (b) diagrams of CRE and CDWRE processes for f = 6, P_{tj} = 5 MPa, P_e = 100 kPa

Results on the rocket engine specific impulse, I_{sp}^{RE}, in f-P_{tj} coordinates are shown in Fig. 3 for CRE and in Fig. 4 for CDWRE. Each figure presents results obtained for P_e = 100 and 1 kPa. CDWRE provides I_{sp} greater by 400-500 m/s at P_e = 100 kPa and by 100-200 m/s at P_e = 1 kPa. At a high P_{tj}, I_{sp} exhibits a maximum in the explored range of f. Comparing these results, one can find that the specific impulse of CDWRE is higher by 8-24 % at sea level and by 2-7 % in vacuum. The highest advantage is obtained for the stoichiometric mixture and the minimum injection pressure. For the case P_e = 1 kPa, let us consider the same I_{sp} of 4800 m/s for both engines. With CRE, this performance is obtained at relatively low f and high P_{tj}, whereas CDWRE offers a possibility to reach the same performance at greater f and much lower P_{tj}.

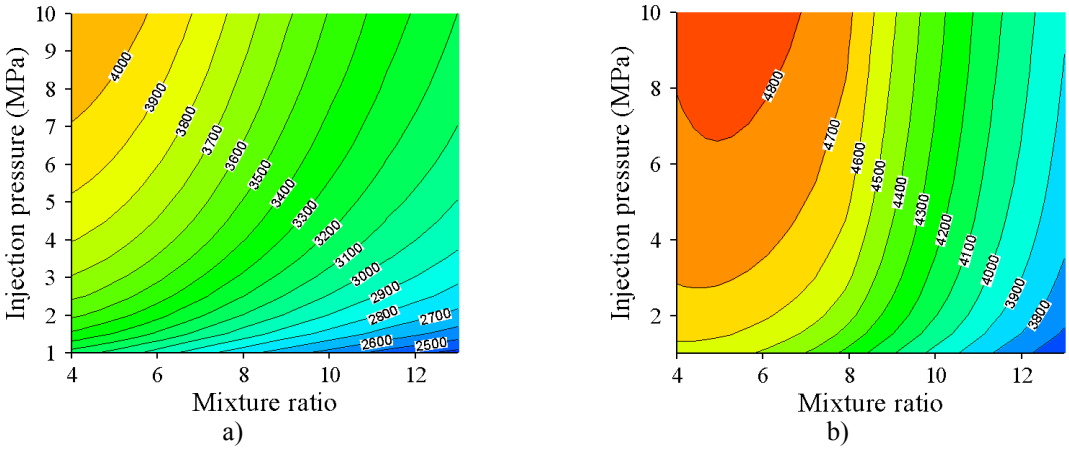

Figure 3: CRE specific impulse in m/s for P_e = 100 kPa (a) and P_e = 1 kPa (b)

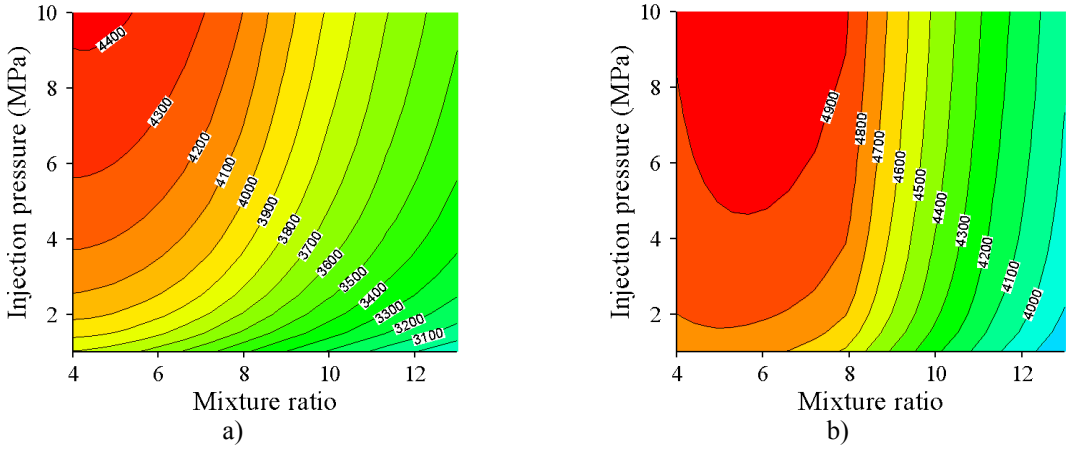

Figure 4: CDWRE specific impulse in m/s for P_e = 100 kPa (a) and P_e = 1 kPa (b)

These results clearly demonstrate important theoretical advantage of CDWRE over CRE. Practical realization of this advantage can significantly improve rocket-based propulsion systems. Several possibilities can be proposed for such an improvement:

– realize a CDWRE with the same operational parameters as a CRE taking benefit of higher specific impulse;
– realize a CDWRE with the same specific impulse by reducing the injection pressure or increasing the mixture ratio; both changes in operational parameters will result in lighter and more compact propulsion systems.

3.2 Kerosene-fuelled turbojet

An airbreathing kerosene-fuelled turbojet is considered in this study. The air composition is specified as 21% of O_2 and 79% of N_2 by volume. The fuel is represented by $C_{10}H_{20}$, whose enthalpy is corrected to have the same calorific value as the aviation kerosene. For equilibrium combustion products, the following set of chemical species is used: H_2, H, O_2, O, OH, H_2O, CO, CO_2, N_2, NO. Performance results are obtained for the ground conditions: flight speed $u_a = 0$; $P_{t\,in}$ = 1 atm; $T_{t\,in}$ =288 K. Kerosene is injected at 300 K, and the fuel equivalence ratio is ϕ = 0.3, 0.4, and 0.5. The total pressure recovery in the combustion chamber is σ_c = 0.95. The compressor-turbine transmission efficiency is η_{tr} = 0.99. The nozzle exit pressure is P_e = 1 atm. Three levels of compressor pressure ratio are taken for the analysis. They are given in Table 1 together with corresponding values of the compressor and turbine efficiency.

Table 1: Parameters of the compressor and turbine

π_{co}	5	10	20
η_{co}	0.88	0.86	0.84
η_{tu}	0.92	0.91	0.90

Thermodynamic cycles for conventional (CTJ) and continuous detonation (CDWTJ) engines are presented in Fig. 5 in *P-v* and *T-s* coordinates. These results are obtained for $\phi = 0.4$ and $\pi_{co} = 10$. The points in the graphs mark gas states in the main cross sections with corresponding designations. States "in" and "co" are identical for both engines and represent total conditions. The difference between the "co" and "m" states is due to the fuel addition and, for CDWTJ, due to the mixture expansion to $M_m = 0.5$. States "d", "c", "th", and "e" have the same meaning as for the rocket engine (see Fig. 2). State "tu" represents total conditions at the turbine exit. As for the rocket engine, additional work is obtained due to compression by detonation, and the detonation-based cycle generates less entropy.

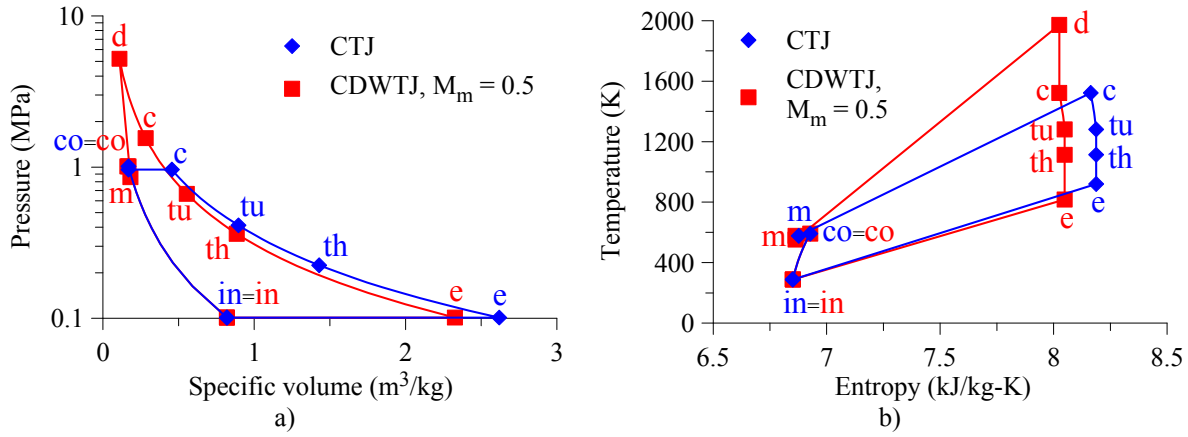

Figure 5: *P-v* (a) and *T-s* (b) diagrams of CTJ and CDWTJ cycles for $\phi = 0.4$ and $\pi_{co} = 10$

Results on specific fuel consumption, C_F^{TJ}, of CTJ and CDWTJ for different π_{co} and ϕ are presented in Fig. 6. The performance of CDWTJ is calculated for two Mach numbers of the fresh mixture flow: $M_m = 0.5$ and 1. Stronger expansion results in lower pressures before and after the detonation and, consequently, in a higher fuel consumption to produce the same thrust. In both cases, however, CDWTJ is more efficient than CTJ. For example, at $\pi_{co} = 10$ and $\phi = 0.4$, the reduction in fuel consumption is 7-12 %. One can see from Fig. 6a that, at a fixed ϕ, CDWTJ is relatively more efficient at lower π_{co}. On the other hand, the trends in Fig. 6b show that, at a fixed π_{co}, the advantage CDWTJ increases with ϕ.

A more pertinent analysis can be provided assuming the same thrust for CTJ and CDWTJ. Taking as a reference the thrust produced by CTJ at $\phi = 0.4$ and using the same compressor with $\pi_{co} = 10$ for both engines, the estimated decrease in fuel consumption for CDWTJ is 11-19 %. Additional fuel economy is obtained due to a lower value of ϕ, which is also beneficial as the turbine thermal load is reduced. Another possibility is to take $\phi = 0.4$ for both engines and to evaluate the difference of π_{co}. With respect to the classical turbojet with $\pi_{co} = 20$, CDWTJ needs 2-3 times lower compression ratio offering possible reduction of the engine mass (less compressor stages, lower mechanical loads on the shaft).

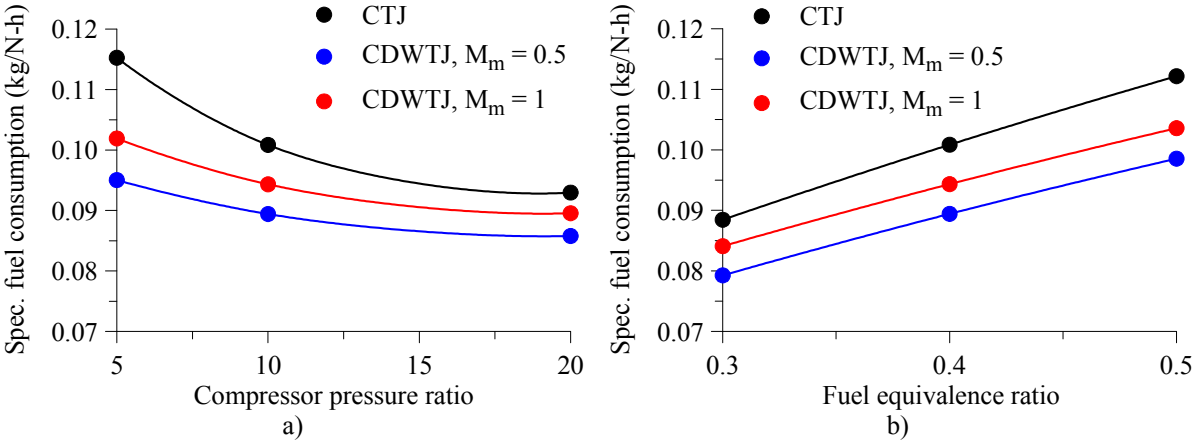

Figure 6: Specific fuel consumption of CTJ and CDWTJ cycles for $\phi = 0.4$ (a) and $\pi_{co} = 10$ (b)

The present results on CDWTJ should be considered as purely theoretical as they do not provide any proof concerning the detonability of air-kerosene mixture under the considered conditions.

4. Conclusion

This study provided comparative theoretical analysis on rocket and turbojet engines operating in the conventional constant-pressure mode and the continuous detonation wave mode. Using global models, based on accurate thermodynamic description of equilibrium combustion products, performance results are obtained in a large domain of operational parameters. Engine cycles are compared providing clear illustration of additional work generated by the CDWE cycle. It follows from the present analysis that, due to this advantage, propulsion systems can be significantly improved by using CDWE. The main challenge in practical realization of CDWE is to minimize pressure losses so they do not overwhelm the compression effect of detonation.

Acknowledgement

This work is financially supported by CNRS and MBDA France.

References

[1] Zeldovich, Y. B. 2006. To the question of energy use of detonation combustion. *J. Propulsion and Power.* 22(3):588-592.
[2] Wintenberger, E. and Shepherd, J. E. 2006. Thermodynamic Cycle Analysis for Propagating Detonations. *Journal of Propulsion and Power*, 22(3):694-697.
[3] Voitsekhovsky, B. V. 1956. Maintained detonations. *Soviet Phys. Dokl.* 4(6):1254-1256 (in Russian).
[4] Voitsekhovskii, B. V. 1960. Stationary spin detonation. *J. Appl. Mech. Techn. Phys*. 3:157-164 (in Russian).
[5] Nicholls, J. A. and Cullen, R. E. 1964. The feasibility of a rotating detonation wave rocket motor. Report of the University of Michigan. RPL-TDR-64-113.
[6] Adamson, T. C., Jr. and Olsson, G. R. 1967. Performance analysis of a rotating detonation wave rocket engine. *Astronautica Acta.* 13(4):405-415.
[7] Bykovskii, F. A. and Mitrofanov, V. V. 1980. Detonative combustion of gas mixture in a cylindrical chamber. *Combustion Explosion and Shock Waves.* 16(5):107-117.
[8] Bykovskii, F. A., Zhdan, S. A., and Vedernikov, E. F. 2006. Continuous spin detonations. *J. Propulsion and Power*. 22:1204-1216.
[9] Davidenko D., Eude Y., Gökalp I., and Falempin F. 2011. Theoretical and numerical studies on continuous detonation wave engines. AIAA-2011-2334. *17th AIAA International Space Planes and Hypersonic Systems and Technologies Conference.*
[10] Gardiner, W. C. 1984. Combustion Chemistry. Springer-Verlag. New York.
[11] Reynolds, W. C. 1986. The Element Potential Method for Chemical Equilibrium Analysis: Implementation in the Interactive Program STANJAN Version 3. Stanford University Report.
[12] Eude Y., Davidenko D., Gökalp I., and Falempin F. 2011. Numerical simulation and analysis of a 3D continuous detonation under rocket engine conditions. *4th European Conference for Aerospace Sciences*.
[13] Eude Y., Davidenko D., Gökalp I., and Falempin F. 2011. Use of the adaptive mesh refinement for 3D simulations of a CDWRE (Continuous Detonation Wave Rocket Engine). AIAA-2011-2236. *17th AIAA International Space Planes and Hypersonic Systems and Technologies Conference.*
[14] Davidenko, D., Gökalp, I., and Kudryavtsev, A. 2008. Numerical study of the continuous detonation wave rocket engine. AIAA 2008-2680. *15th AIAA International Space Planes and Hypersonic Systems and Technologies Conference*.
[15] Davidenko, D. M., Gökalp, I., and Kudryavtsev, A. N. 2010. Numerical simulation of continuous detonation in a layer of hydrogen-oxygen mixture with periodic conditions. In: *Deflagrative and detonative combustion*, G. Roy and S. Frolov (eds.). Torus Press, Moscow. 407-422.
[16] Fickett, W. and Davis, W. C. 1979. Detonation. University of California Press.